

A Power Relay System With Multiple Loads Using Asymmetrical Coil Design

Chenwen Cheng , Zhe Zhou , Weiguo Li, Zhanfeng Deng, and Chunting Chris Mi , *Fellow, IEEE*

Abstract—In this article, we propose a power relay system to power multiple loads wirelessly via magnetic coupling. Multiple power relays are placed in a line and the power can be transferred between these relays. Each power relay consists of two relay coils, which function as the receiver and transmitter, respectively. In order to suppress the magnetic coupling between the two relay coils in the same power relay, bipolar coils are adopted and placed perpendicularly. A compensation capacitor is connected in series with each transmitting coil, while another one is connected in parallel with each receiving coil. It is derived that the constant voltage characteristics can be obtained for each load, which means the load power is decoupled from each other. The two coils in the same power relay have different inductance values, which form an asymmetrical structure to achieve equal load voltage distribution. Moreover, zero phase angle can be obtained for the input impedance. The proposed system is suitable to power the gate drivers of series-connected insulated gate bipolar transistors, where multiple isolated power supplies are needed. An experimental prototype with six loads has been constructed to validate the proposed system. The maximum efficiency can reach 94.0% at a power level of 12.6 W.

Index Terms—Asymmetrical coil structure, constant voltage (CV) output, multiple loads, power relay, wireless power transfer (WPT).

I. INTRODUCTION

IN HIGH-VOLTAGE applications, series-connected insulated gate bipolar transistors (IGBTs) are usually used to control the power flow because the voltage rating of a single IGBT is not large enough [1]. Isolated power supplies are necessary for these IGBTs because they have different reference potentials. Moreover, a high insulation level is required for these isolated power supplies to ensure safety.

Manuscript received September 11, 2019; revised November 27, 2019 and December 14, 2019; accepted January 9, 2020. Date of publication February 5, 2020; date of current version October 30, 2020. This work was supported by Global Energy Interconnection Research Institute Company Ltd. (GEIRI), under Grant GEIRI-DL-71-17-011 (State Grid Sci and Tech Project: Research on the Magnetic-Resonant Wireless Power Transfer Technology for the High-Voltage Converter Valve in FACTS). (Corresponding author: Chunting Chris Mi.)

C. Cheng and C. C. Mi are with the San Diego State University, San Diego, CA 92182 USA (e-mail: cheng.cwen@gmail.com; mi@ieee.org).

Z. Zhou, W. Li, and Z. Deng are with the State Key Laboratory of Advanced Power Transmission Technology, Global Energy Interconnection Research Institute, Beijing 102211, China (e-mail: zhouzhe@geiri.sgcc.com.cn; lwgmb90549@sina.com; iphone21@sina.com).

Color versions of one or more of the figures in this article are available online at <https://ieeexplore.ieee.org>.

Digital Object Identifier 10.1109/TIE.2020.2970636

The high insulation transformer can be used to provide isolated power supplies for driver circuits, which are usually bulky and costly [2]. In [3], a self-supplied gate driver was designed for the silicon-controlled rectifier, which obtained the power directly from the power switch. Unfortunately, such a technology cannot be applied in other applications [3]. The bootstrap method provides another solution to power the driver circuit for the high-side switch [4]. However, this method is limited to the low-power application and not suitable for more IGBTs connected in series. In [5], the gate power was supplied from the main circuit in the modular multilevel converter. However, this method cannot provide a stable power supply for the gate driver during a power outage. Thus, a method independent of the main circuit need to be designed to provide multiple isolated power supplies for the gate drivers of series-connected IGBTs.

The wireless power transfer (WPT) technology provides another solution to power the gate drivers [6]–[9]. Since no direct contact is needed between the transmitter and the receiver, a high insulation level can be achieved. An isolated gate drive power supply for the medium-voltage converters was presented in [6] and [7] using the WPT technology. However, the designed system can only power one load. Another WPT system was designed for the six gate drivers in a three-phase inverter in [8] and [9]. In order to avoid the cross coupling between different receiving coils, these receiving coils should be placed with enough space. In [10], the efficiency and electromagnetic interference analysis of the WPT system for a high-voltage gate driver application was analyzed. However, only one driver can be powered. In order to power multiple gate drivers simultaneously, a WPT system with one transmitting coil and one receiving coil was designed in [11]. However, the insulation level between these driver circuits is low because there is no galvanic isolation between them. Another topology adopted multiple transmitter–receiver pairs to power the gate drivers in [12]. The transmitters are connected in series so that the working condition of each load will affect each other.

In [13], a WPT system adopting many coils in a domino form was applied to power multiple loads over a long distance. However, the load power depends on each other, which increases the power control complexity. In order to solve the power control difficulty, a novel WPT system based on the multiple power relays was designed in [14] and [15]. Each relay contains two identical coils, which have the same inductance value and form a symmetrical relay structure. With the CLC [14] or SPS [15] compensation method, the constant current (CC) can be obtained for each load. Thus, the load power variation will not affect

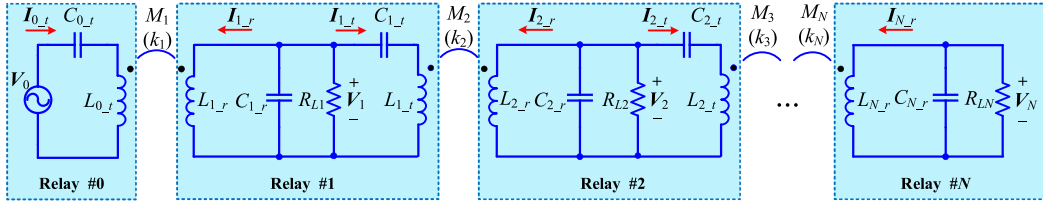


Fig. 1. System topology of the multiloading power relay system.

each other. However, usually, a constant voltage (CV) source is required for the gate driver circuit. For example, a 15 V dc voltage source is used to turn an IGBT ON and a -8 V dc voltage source is used to turn it OFF. Thus, the WPT systems in [14] and [15] cannot be directly applied to power the gate drivers. An additional conversion circuit should be used to transform the CC output to a CV, which increases the system complexity.

Based on the above discussion, a novel multiloading WPT system is proposed to power the gate drivers of series-connected IGBTs. The main contributions of this article are shown as follows.

- 1) The proposed WPT system can power multiple loads with CV outputs so that the load power will not affect each other, which is especially suitable to power the gate drivers of series-connected IGBTs.
- 2) The power relay that consists of two relay coils, i.e., the transmitting coil and the receiving coil, is designed to power the load. The two coils in the same power relay have different inductances and an asymmetrical relay structure is formed, which helps obtain equal load voltage distribution among all the loads.
- 3) Only two capacitors are used for each power relay and no compensation inductor is needed. Thus, the compensation circuit is much simpler than those in [14] and [15].

An experimental setup with six loads has been designed to validate the proposed system. The maximum system efficiency can reach 94.0% at a power level of 12.6 W.

II. SYSTEM DESCRIPTION

A. System Modeling

In the proposed wireless power relay system, the intermediate relay coils are used to power N loads, as shown in Fig. 1. The Power Relay $\#n$ ($n = 1, 2, \dots, N - 1$) that consists of two relay coils transmits power not only to the local load connected to it but also to the next relay. One of the two relay coils in Relay $\#n$, marked as $L_{n,r}$, receives power from its previous relay, while the other coil, marked as $L_{n,t}$, transmits power to the next relay. In Relay $\#0$, only the transmitting coil $L_{0,t}$ exists, which is connected to the high-frequency ac source V_0 and transmits power to Relay $\#1$. Relay $\#N$ only contains the receiving coil $L_{N,r}$ and receives power from Relay $\#(N - 1)$. The compensation capacitor $C_{n,t}$ is connected in series with $L_{n,t}$ ($n = 0, 1, 2, \dots, N - 1$) and $C_{n,r}$ is connected in parallel with $L_{n,r}$ ($n = 1, 2, \dots, N$) in each relay. The load is connected across $C_{n,r}$ in Relay $\#1$ – $\#N$. In practical applications, a rectifier should be used to transform the received ac power to a dc voltage source for the gate drivers. Considering that the

input voltage across the rectifier and the current flowing through the rectifier are in phase, the rectifier together with the real load can be modeled as a load resistor R_{Ln} ($n = 1, 2, \dots, N$) [14]. Although there are multiple coils in the proposed system, only the magnetic coupling between $L_{n-1,t}$ and $L_{n,r}$ needs to be considered, as shown in Fig. 1, because of the coil structure discussed in Section II-D. The coupling coefficient and the corresponding mutual inductance between $L_{n-1,t}$ and $L_{n,r}$ are defined as k_n and M_n , respectively, which has the following relationship:

$$k_n = M_n / \sqrt{L_{n-1,t} \cdot L_{n,r}}. \quad (1)$$

B. CV Outputs

The circuit model of the proposed power relay system can be obtained based on the T-model of the loosely coupled transformer, as shown in Fig. 2. $I_{n,r}$ and $I_{n,t}$ are the currents flowing through $L_{n,r}$ and $L_{n,t}$, respectively, ($n = 0, 1, 2, \dots, N$); V_n ($n = 1, 2, \dots, N$) is the load voltage across R_{Ln} . The positive direction of these currents and voltages is defined, as shown in Fig. 2. $r_{n,t}$ and $r_{n,r}$ are the parasitic resistances of the corresponding coils.

In order to facilitate the analysis and the derivation of the resonant conditions achieving CV outputs and the zero phase angle (ZPA) of the input impedance, the mutual inductance M_n can be regarded as the parallel connection of an inductor L_{nx} and a capacitor C_{nx} , which should meet the following condition:

$$M_n = L_{nx} / (1 - \omega_0^2 L_{nx} C_{nx}) \quad (2)$$

where ω_0 is the operating angular frequency. In this section, the coils' parasitic resistances are neglected initially to simplify the analysis, whose influence on the system performance will be analyzed in Section III. As can be seen from Figs. 1 and 2, the proposed power relay system can be regarded as multiple transmitter–receiver pairs connected in cascade. The n th transmitter–receiver pair consisting of $L_{n-1,t}$ and $L_{n,r}$ in Fig. 2 is redrawn in Fig. 3.

In Fig. 3, the series connection of the compensation capacitor $C_{n-1,t}$ and the inductor ($L_{n-1,t} - M_n$) can be modeled as a new capacitor $C'_{n-1,t}$, which can be calculated as

$$C'_{n-1,t} = C_{n-1,t} / [1 - \omega_0^2 (L_{n-1,t} - M_n) \cdot C_{n-1,t}]. \quad (3)$$

According to [16], a CC source can be obtained from the input voltage source V_{n-1} , if $C'_{n-1,t}$ resonates with L_{nx} , i.e.,

$$\omega_0^2 = 1 / (L_{nx} \cdot C'_{n-1,t}). \quad (4)$$

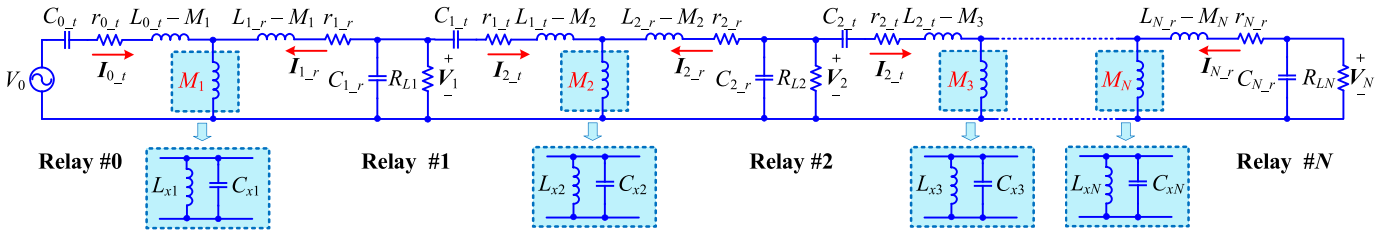


Fig. 2. Circuit model of the proposed multiload power relay system.

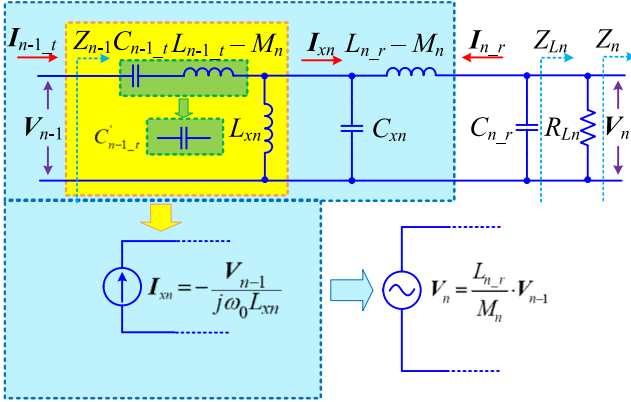


Fig. 3. Equivalent circuit model of the n th transmitter-receiver pair.

The equivalent CC source I_{xn} can be calculated as

$$I_{xn} = -V_{n-1}/(j\omega_0 L_{xn}). \quad (5)$$

Thevenin's theorem can be used to further simplify Fig. 3. First, the current source I_{xn} is regarded as open when calculating the internal impedance. It can be found that C_{xn} and $(L_{n,r} - M_n)$ are connected in series. If C_{xn} resonates with $(L_{n,r} - M_n)$, the internal impedance is zero, which means Thevenin equivalent circuit is a voltage source [16], i.e.,

$$\omega_0^2 = 1/[(L_{n,r} - M_n) \cdot C_{xn}]. \quad (6)$$

Based on (2), L_{xn} can be rewritten as

$$L_{xn} = \frac{M_n}{1 + \omega_0^2 C_{xn} M_n} = \frac{M_n(L_{n,r} - M_n)}{L_{n,r}}. \quad (7)$$

In order to calculate the open-circuit voltage, the output should be disconnected from $C_{n,r}$ and Z_{Ln} and the output voltage will be exactly that of the ideal voltage source. In this case, the current I_{xn} will all flow through C_{xn} . Thus, the open-circuit output voltage can be calculated as

$$V_n = \frac{I_{xn}}{j\omega_0 C_{xn}} = \frac{L_{n,r} - M_n}{L_{xn}} \cdot V_{n-1} = \frac{L_{n,r}}{M_n} \cdot V_{n-1}. \quad (8)$$

It can be seen from (8) that the constant load voltage V_n can be obtained if the input voltage V_{n-1} is constant. The load voltage is inversely proportional to the mutual inductance M_n . The resonant conditions can be simplified further by submitting (7) into (4) as

$$\omega_0^2 \cdot (L_{n-1,t} - M_n^2/L_{n,r}) \cdot C_{n-1,t} = 1. \quad (9)$$

When the input voltage V_0 of the proposed power relay system is constant, it can be derived that all the load voltages are constant regardless of the load resistance when neglecting the parasitic resistances. Thus, the load power can be regulated flexibly and independently, which greatly decreases the power control design. Moreover, all the load voltages are identical, i.e., $V_1 = V_2 = \dots = V_N$, when the following condition is met:

$$L_{n,r} = M_n, \quad n = 1, 2, 3, \dots, N. \quad (10)$$

C. ZPA of Input Impedance

In real applications, the ZPA of the input impedance is important to minimize the inverter's volt-ampere rating. In Fig. 3, the equivalent impedance of the subsequent circuit after R_{Ln} is defined as Z_n and the input impedance is defined as Z_{n-1} . The parallel-connection circuit of R_{Ln} and Z_n is assumed to be Z_{Ln} , which can be calculated as

$$Z_{Ln} = R_{Ln} \cdot Z_n / (R_{Ln} + Z_n). \quad (11)$$

Then, the input impedance Z_{n-1} can be calculated according to Fig. 3 as

$$Z_{n-1} = \frac{\omega_0^2 M_n^2 Z_{Ln} + j\omega_0 \frac{Z_{Ln}^2 M_n^2 (1 - \omega_0^2 L_{n,r} C_{n,r})}{L_{n,r}}}{(Z_{Ln} - \omega_0^2 L_{n,r} C_{n,r} Z_{Ln})^2 + (\omega_0 L_{n,r})^2}. \quad (12)$$

It can be seen from (12) that when Z_{Ln} is resistive, which means Z_n is resistive, Z_{n-1} is also resistive if the following condition is met:

$$\omega_0^2 \cdot L_{n,r} \cdot C_{n,r} = 1. \quad (13)$$

In this case, Z_{n-1} can be simplified as

$$Z_{n-1} = M_n^2 \cdot Z_{Ln} / L_{n,r}^2. \quad (14)$$

Considering that $Z_{Ln} = R_{Ln}$ in the Relay # N is resistive, Z_n ($n = 0, 1, 2, \dots, N - 1$) can be derived based on (14) to be resistive in each relay. Based on (9) and (13), the values of the series- and parallel-compensated capacitors can be determined, which not only obtain the constant load voltage for each load but also ensure the ZPA of the total input impedance.

D. Coil Design

Although there are many coils in the proposed power relay system, as shown in Fig. 1, only the magnetic coupling between $L_{n-1,t}$ and $L_{n,r}$ is desirable, while the coupling between any other coils should be as small as possible in order to obtain the CV outputs based on the above-mentioned analysis. To meet

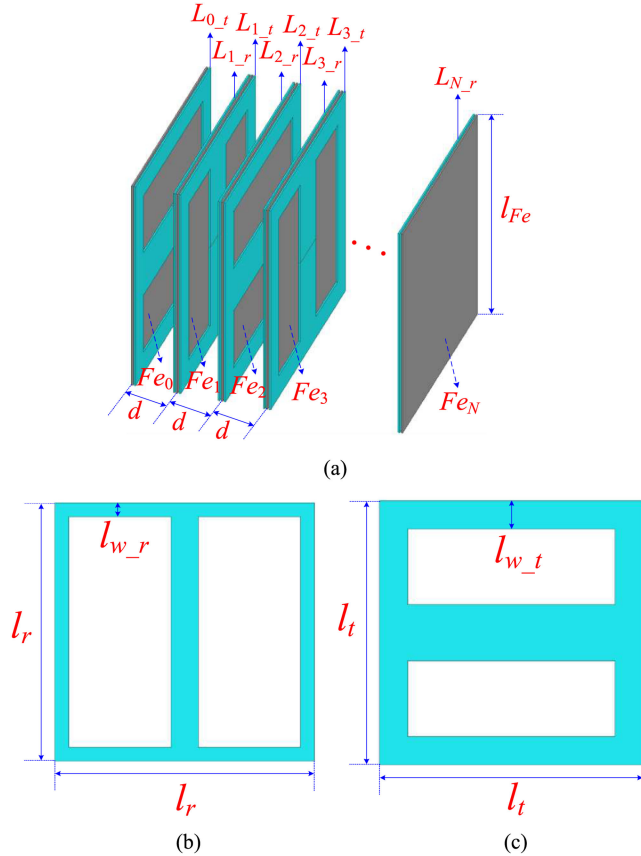


Fig. 4. Asymmetrical coil structure and dimension of the proposed power relay system. (a) Coil structure. (b) Receiving coil. (c) Transmitting coil.

this requirement, a feasible coil structure is designed, as shown in Fig. 4(a). All the coils are bipolar, as shown in Fig. 4(b) and (c). The two bipolar relay coils in Relay # n are placed perpendicularly so that the magnetic coupling between them can be neglected [14]. In Relay # n ($n = 1, 2, \dots, N-1$), a ferrite plate Fe_n is inserted between $L_{n,r}$ and $L_{n,t}$. In Relay #0 or # N , the ferrite plate Fe_0 or Fe_N is also placed besides $L_{0,t}$ or $L_{N,r}$. The ferrite plate Fe_n can suppress the undesirable coupling between the two coils in the same power relay and any other nonadjacent coils. Moreover, the magnetic coupling k_n between $L_{n-1,t}$ and $L_{n,r}$ can be enhanced, which is beneficial for improving the power transfer capability.

In order to verify the proposed coil structure, a design example is given using Maxwell. The distance between two adjacent relays is set as $d = 30$ mm, which is considered as the distance between two IGBTs. Theoretically, this distance can withstand a voltage as high as 90 kV, considering the breakdown voltage of dry air is 3 kV/mm. The receiving coil, the transmitting coil, and the ferrite plate are all squares with the identical side length $l_r = l_t = l_{Fe} = 150$ mm. All receiving coils have the same inductance value, so do the transmitting coils. The mutual inductances and the corresponding coupling coefficients between any two adjacent power relays are also identical because

TABLE I
SIMULATED COUPLING COEFFICIENTS

$k_{1r,1t}$	$k_{1r,2r}$	$k_{1r,2t}$	k_2	$k_{1t,2r}$
0.0002	0.00004	0.0059	0.4801	0.00005

the distance between them is the same, i.e.,

$$\begin{aligned} L_{1,r} &= L_{2,r} = \dots = L_{N,r} = L_r, \\ L_{1,t} &= L_{2,t} = \dots = L_{N,t} = L_t \end{aligned} \quad (15)$$

$$\begin{aligned} M_1 &= M_2 = \dots = M_N = M, \\ k_1 &= k_2 = \dots = k_N = k. \end{aligned} \quad (16)$$

The identical load voltage for each load is desirable in this design example because the gate drivers are the same so that the identical driving voltage is needed. Thus, the condition in (10) should be met, which means $L_r = M$. Thus, the coupling coefficient in (1) can be rewritten as

$$k = M / \sqrt{L_r \cdot L_t} = \sqrt{L_r / L_t} < 1. \quad (17)$$

Considering that the coupling coefficient k is usually smaller than 1, the inductance of the receiving coil L_r should be smaller than that of the transmitting coil L_t , i.e., $L_r < L_t$. It means an asymmetrical relay structure is needed in the proposed system to obtain equal load voltage distribution. Thus, the coil width of the receiving coil $l_{w,r} = 8$ mm is designed to be smaller than that of the transmitting coil $l_{w,t} = 16$ mm, as shown in Fig. 4(b) and (c). In order to reduce the calculation burden of the computer, only two adjacent relays are simulated because all the power relays have the same structure and dimension. Taking Relays #1 and #2 for example, the coupling coefficients between $L_{1,r}$ and $L_{1,t}$, $L_{1,r}$ and $L_{2,r}$, $L_{1,r}$ and $L_{2,t}$, and $L_{1,t}$ and $L_{2,t}$ are defined as $k_{1r,1t}$, $k_{1r,2r}$, $k_{1r,2t}$, k_2 , and $k_{1t,2t}$, respectively, which has been listed in Table I.

It can be seen from Table I that $k_{1r,1t}$, $k_{1r,2r}$, $k_{1r,2t}$, and $k_{1t,2t}$ are very small compared with k_2 so that they can be neglected. Thus, the designed coil structure is suitable for the proposed multiload power relay system.

III. POWER TRANSFER CAPABILITY

In a practical application, the coils' parasitic resistances are inevitable, the influence of which on the system performance will be analyzed in this section. Assuming that the quality factors of coils $L_{n,r}$ and $L_{n,t}$ are $Q_{n,r}$ and $Q_{n,t}$, respectively, the parasitic resistances $r_{n,r}$ and $r_{n,t}$ can be calculated as

$$r_{n,r} = \omega_0 L_{n,r} / Q_{n,r}, \quad r_{n,t} = \omega_0 L_{n,t} / Q_{n,t}. \quad (18)$$

According to the coil structure in Section II-D, the quality factors of all the receiving coils or the transmitting coils are identical, i.e.,

$$\begin{cases} Q_{1,r} = Q_{2,r} = \dots = Q_{N,r} = Q_r \\ Q_{0,t} = Q_{2,t} = \dots = Q_{N-1,t} = Q_t \end{cases}. \quad (19)$$

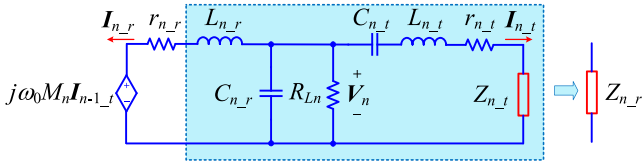


Fig. 5. Reflection impedances in Relay # n .

A. Reflection Impedance

In order to facilitate the system analysis when considering the coils' parasitic resistances, the concept of the reflection impedance is used here. The reflection impedance in each coil is defined as the equivalent impedance of the whole circuits following the specific coil, which can be used to model these circuits. Fig. 5 illustrates the reflection impedances $Z_{n,r}$ and $Z_{n,t}$ in coils $L_{n,r}$ and $L_{n,t}$ of Relay # n ($n = 1, 2, \dots, N - 1$), which can be calculated as

$$\begin{cases} Z_{n,t} = (\omega_0 M_{n+1})^2 / (r_{n+1,r} + Z_{n+1,r}) \\ Z_{n,r} = \frac{(\omega_0 L_{n,r})^2}{\frac{1}{j\omega_0 C_{n,r}} + \frac{R_{Ln} \left(\frac{j\omega_0 M_{n+1}^2}{L_{n+1,r}} + r_{n,t} + Z_{n,t} \right)}{R_{Ln} + \frac{j\omega_0 M_{n+1}^2}{L_{n+1,r}} + r_{n,t} + Z_{n,t}}} \end{cases} \quad (20)$$

For Relay # N , only $Z_{N,r}$ exists because there is no transmitting coil, which can be calculated as

$$Z_{N,r} = (\omega_0 L_{N,r})^2 / (R_{LN} - j\omega_0 L_{N,r}). \quad (21)$$

The reflection impedance $Z_{0,t}$ in coil $L_{0,t}$ can also be calculated using (20). Then, the input impedance Z_{in} of the whole system from the view of the inverter can be calculated as $Z_{in} = r_{0,t} + Z_{0,t}$. Fig. 6 shows the phase angle variation of Z_{in} against the increasing load power in one relay, where $k = 0.49$, $Q = 200$, $Q_f = 150$, and $N = 6$, which has been normalized by dividing its base value P_b , which can be calculated as

$$V_b = V_0, \quad R_b = \omega_0 M, \quad P_b = V_b^2 / R_b. \quad (22)$$

All the load resistances are identical here, i.e.,

$$R_{L1} = R_{L2} = \dots = R_{LN} = R_L. \quad (23)$$

It should be pointed out that the proposed power relay system can still work with different loads. The condition in (23) is not necessary, which is used just to facilitate the analysis. Moreover, nearly equal power distribution can be achieved if the load voltages do not vary too much.

The load power in Relay # n can be calculated as $P_{Ln} = V_n^2 / R_{Ln}$. The load voltage V_n is assumed to drop slightly, which is basically equal to V_0 , and can be verified from Fig. 7. Then, the normalized load power can be approximated as

$$P_{Ln_norm} = P_{Ln} / P_b \approx R_b / R_L. \quad (24)$$

So, the x -axis in Fig. 6 is R_b / R_L , which is a pure number (per unit value) and approximately the normalized load power. It can be seen from Fig. 6 that the phase angle of Z_{in} is less

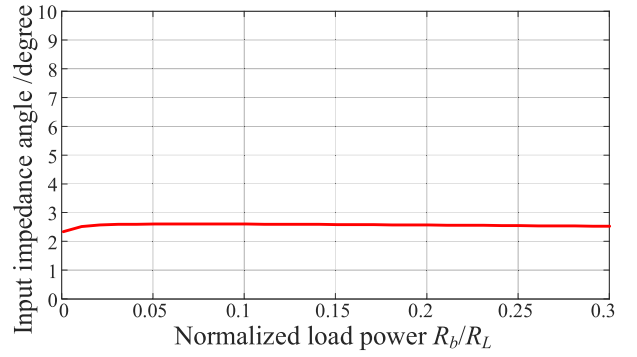


Fig. 6. Phase angle of the input impedance Z_{in} ($k = 0.49$, $Q = 200$, $Q_f = 150$, and $N = 6$).

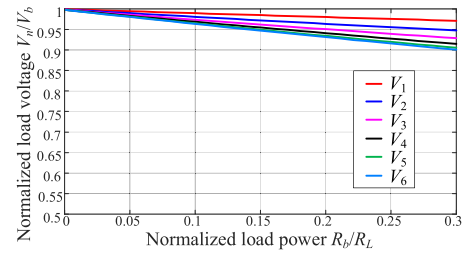


Fig. 7. Load voltage variations against the increasing load power ($k = 0.49$, $Q_t = 200$, $Q_r = 150$, and $N = 6$).

than 3° , which is very small. Thus, Z_{in} is basically resistive, and the coils' parasitic resistances introduce only a small amount of reactive power in the system. According to the efficiency curve in the experimental part, the optimum normalized load power is within $[0.1, 0.3]$ to ensure high efficiency and good constant load voltage characteristics.

B. Load Voltage

Based on the reflection impedances, as shown in (20), the load voltages can be calculated when considering the parasitic resistances. In Relay # n ($n = 1, 2, \dots, N - 1$), $I_{n,r}$, V_n , and $I_{n,t}$ can be calculated according to Fig. 5 as

$$\begin{cases} I_{n,r} = -j\omega_0 M_n I_{n-1,t} / (r_{n,r} + Z_{n,r}) \\ V_n = j\omega_0 M_n I_{n-1,t} + I_{n,r} \cdot (r_{n,r} + j\omega_0 L_{n,r}) \\ I_{n,t} = V_{Ln} / [1 / (j\omega_0 C_{n,t}) + j\omega_0 L_{n,t} + r_{n,t} + Z_{n,t}] \end{cases} \quad (25)$$

$V_{N,r}$ and V_N in Relay # N can also be calculated based on (25). In Relay #0, $I_{0,t}$ in transmitting coil $L_{0,t}$ is

$$I_{0,t} = V_0 / Z_{in}. \quad (26)$$

Then, the load voltages can be calculated iteratively using (25) and (26) beginning with Relay #0. The load voltage variations against the increasing load power are shown in Fig. 7, where the load voltages and power are normalized by dividing their base values in (22). It can be seen from Fig. 7 that when the load power increases, the load voltages decrease gradually because some power is consumed by the parasitic resistance. In

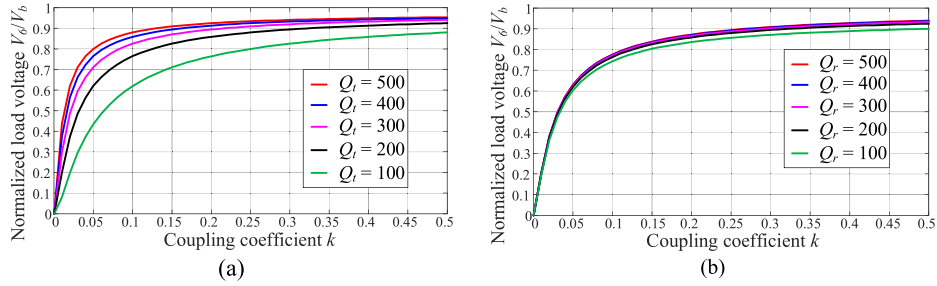


Fig. 8. Variations of the last load voltage V_6 with (a) different coupling coefficients k and quality factors Q_t of the transmitting coil ($Q_r = 200$, $N = 6$, and $R_b/R_L = 0.25$) and (b) different coupling coefficients k and quality factors Q_r of the receiving coil ($Q_t = 200$, $N = 6$, and $R_b/R_L = 0.25$).

an ideal system where the parasitic resistance is zero, the load voltage will be constant regardless of the load. The last load voltage V_N decreases the most. Thus, V_N can be regarded as a criterion for evaluating the CV characteristics of the proposed system.

Fig. 8(a) shows the variation of V_6 against coupling coefficients k with different quality factors Q_t of the transmitting coil, where $Q_r = 200$, $N = 6$, and $R_b/R_L = 0.25$. The quality factor is changed by varying the parasitic resistance. A smaller drop of V_6 is obtained with a larger k or Q_t , as can be seen from Fig. 8(a), which means a better CV characteristic can be achieved. Similar conclusions can be obtained for the quality factor Q_r of the receiving coil from Fig. 8(b).

IV. EXPERIMENTAL VALIDATION

An experimental setup of the proposed power relay system with six loads has been constructed, as shown in Fig. 9. All the coils are made of the Litz wire to decrease the power loss. PC95 is used as the ferrite material. The film capacitor from KEMET is used to compensate the circuit, which is placed next to the power relay. The dimensions of both the coils and the ferrite plates are the same as in the simulation model in Section II-D. An H-bridge inverter made up of four silicon carbide metal-oxide-semiconductor field-effect transistors (MOSFETs) is adopted to generate a high-frequency ac power source to power the whole system. Considering that the optimal operating frequency of PC95 is from 100 to 300 kHz and the maximum withstand voltage of the compensation capacitor drops dramatically when the frequency exceeds 100 kHz, the operating frequency of the inverter is chosen as 200 kHz. Moreover, if the operating frequency is too high, the system can be easily detuned because of the inductance or capacitance variation during operation. The switching loss will also increase at the higher switching frequency.

The detailed system parameters are listed in Table II. The inductance, capacitance, and quality factor are measured using the LCR meter E4980AL from Keysight Technologies. During the experiment, the self-inductance L_{n_r} and L_{n_t} in Relay # n are measured first. Then, the compensation capacitances C_{n_r} and C_{n_t} can be calculated based on (9) and (13). Thus, the compensation capacitance is adjusted based on the real measured inductance value so that each power relay can be adjusted to reach good resonant condition, although there exist parameter differences among different relays.

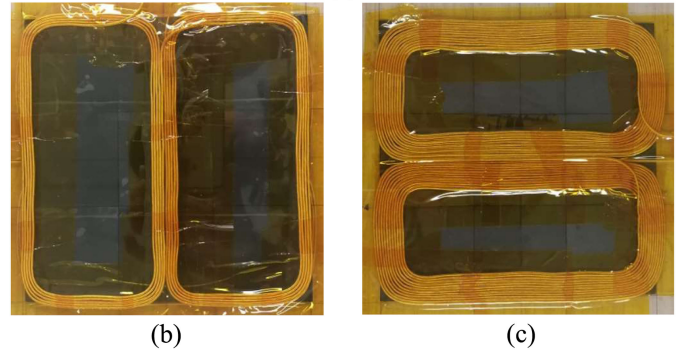
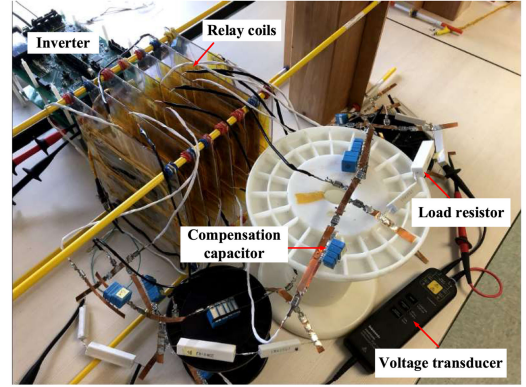


Fig. 9. Experimental setup with six loads. (a) Experimental platform. (b) Receiving coil L_{n_r} . (c) Transmitting coil L_{n_t} .

TABLE II
PARAMETERS OF THE EXPERIMENTAL SYSTEM

Parameter	Value	Parameter	Value
V_{dc}	25 V	f_s	200 kHz
$L_{0_r} \sim L_{5_r}$	120 μ H	$L_{1_r} \sim L_{6_r}$	29.5 μ H
$C_{0_r} \sim C_{5_r}$	7.00 nF	$C_{1_r} \sim C_{6_r}$	21.47 nF
k	0.49	M	29.2 μ H
Q_t	200	Q_r	150

Fig. 10 shows the load voltage waveforms. The inverter's output voltage V_0 is almost in phase with I_{0_t} that flows through L_{0_t} . It means that little reactive power exists, which helps decrease the power rating of the inverter. Moreover, I_{0_t} lags

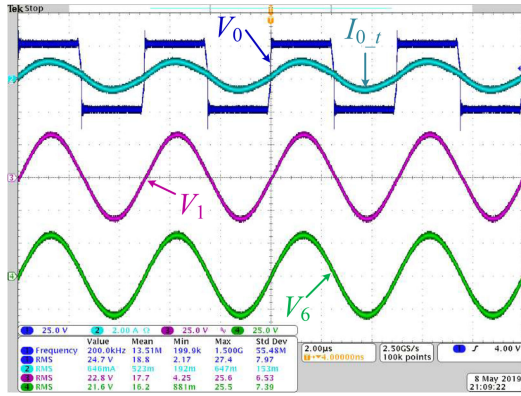


Fig. 10. Experimental load voltage waveforms.

TABLE III
EXPERIMENTAL DATA

V_1	23.8	23.3	22.9	22.8	22.5	22.4	22.2
R_{L1}	∞	705.2	351.9	236.5	171.8	147.2	116.6
V_2	23.8	23.3	22.9	22.6	22.3	22.3	21.7
R_{L2}	∞	697.3	359.1	243.7	171.7	147.3	116.8
V_3	23.8	23.2	22.7	22.4	22.1	21.9	21.2
R_{L3}	∞	701.1	349.8	234	171.3	147.3	116.4
V_4	23.8	23.2	22.5	22.2	21.7	21.5	20.9
R_{L4}	∞	694.2	347.7	232.1	171.7	147.3	115.8
V_5	23.7	23.1	22.4	22.1	21.7	21.3	20.6
R_{L5}	∞	696.5	355	239.2	171.6	147.4	116.9
V_6	23.6	22.9	22.3	21.9	21.3	21	20.4
R_{L6}	∞	699.8	353.7	238.7	172.2	147.4	116.5
P_{in}	0.79	5.25	9.39	13.42	18.01	20.81	25.29
P_o	0	4.61	8.70	12.61	16.82	19.25	23.09
Eff		0.878	0.926	0.940	0.934	0.925	0.913

a little behind V_0 . Thus, zero-voltage switching is achieved for the MOSFETs and the switching loss can be greatly decreased. The load voltages V_1 and V_6 are also given in Fig. 10 that are almost in phase and have the same amplitude, which is consistent with the analysis in Section II.

Table III lists the experimental data including the load powers, load resistance, and load voltages in each load as well as the system efficiency at different power levels. Fig. 11 shows the total load power variations with regard to the increasing load resistance using the experimental data in Table III. It can be seen that the load power is reversely proportional to the load resistance.

The load voltage variation versus the increasing load power is shown in Fig. 12. The load power is altered by changing the load resistance. The solid line represents the calculated load voltages and the dot points represent the measured values in the experiment. The measured values match the calculated ones well with the error within 5%.

Fig. 13 shows the system efficiency variation versus the increasing load power where the solid line is the calculated

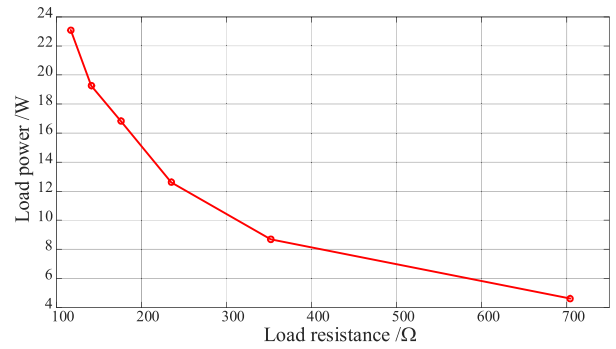


Fig. 11. Total load power variations against the increasing load resistance.

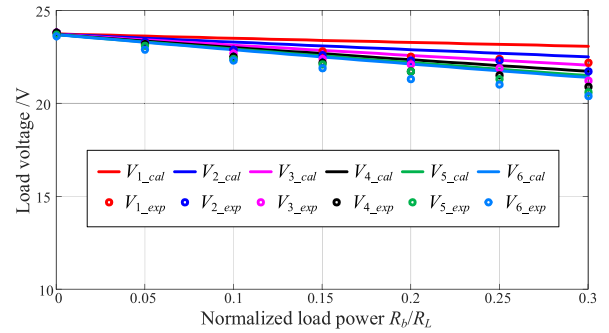


Fig. 12. Experimental load voltage variation against increasing load power.

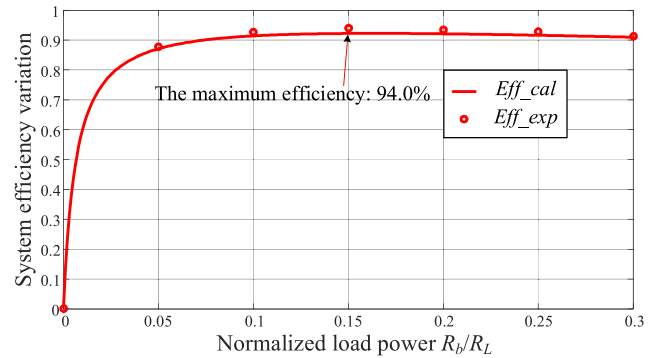


Fig. 13. Variation of the system efficiency against increasing load power.

efficiency. The dotted points are the measured values. The maximum efficiency can reach 94.0% at a total output power of 12.6 W, which is very high considering that there are total six loads in the system. The system efficiency is still as high as 91.3% when the load power is 23.1 W (the normalized load power is 0.3).

Fig. 14 shows the load voltage variation with different loads. The red circles represent the six load voltages where $R_b/R_1 = 0$, $R_b/R_2 = 0.05$, $R_b/R_3 = 0.10$, $R_b/R_4 = 0.15$, $R_b/R_5 = 0.20$, and $R_b/R_6 = 0.25$, while the blue crosses represent the load voltages where $R_b/R_1 = 0.25$, $R_b/R_2 = 0.20$, $R_b/R_3 = 0.15$, $R_b/R_4 = 0.10$, $R_b/R_5 = 0.05$, and $R_b/R_6 = 0$. It can be seen that the load voltages do not vary too much even

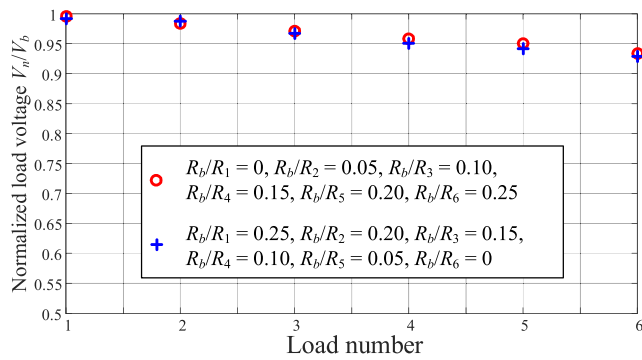


Fig. 14. Load voltage variations with different loads.

with different loads. Thus, the proposed power relay system works well in different load conditions and nearly constant load voltages can be obtained.

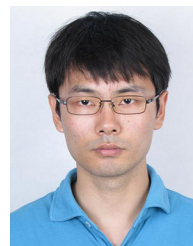
V. CONCLUSION

In this article, a novel power relay system with multiple loads had been proposed using bipolar relay coils. An asymmetrical power relay structure was designed to obtain equal load voltage distribution, which contained two relay coils of different inductances and a ferrite plate. One relay coil received power from its previous power relay and the other one transmitted power to its next power relay. The two relay coils in the same power relay were placed perpendicularly to realize the magnetic decoupling between them. The CV characteristics could be obtained for all the loads with a simple compensation circuit. The influence of the parasitic resistances on the system performance was analyzed, which showed that a larger coupling coefficient between the two adjacent power relays or a larger quality factor of the relay coil leads to a better CV characteristic. The proposed power relay system can be used to power the multiple gate drivers of series-connected IGBTs where multiple isolated power supplies were needed. An experimental prototype with six loads was designed to validate the proposed power relay system. The system can achieve a maximum efficiency of 94.0% at a power level of 12.6 W.

REFERENCES

- [1] F. Zhang, X. Yang, Y. Ren, L. Feng, W. Chen, and Y. Pei, "A hybrid active gate drive for switching loss reduction and voltage balancing of series-connected IGBTs," *IEEE Trans. Power Electron.*, vol. 32, no. 10, pp. 7469–7481, Oct. 2017.
- [2] I. Aizpuru, J. M. Canales, and J. Fernandez, "Scalable high insulation power supply for medium voltage power converters," in *Proc. 7th Int. Conf. Integr. Power Electron. Syst.*, Mar. 2012, pp. 1–6.
- [3] D. M. Raonic, "SCR self-supplied gate driver for medium-voltage application with capacitor as storage element," *IEEE Trans. Ind. Appl.*, vol. 36, no. 1, pp. 212–216, Jan./Feb. 2000.
- [4] S. Park and T. M. Jahns, "A self-boost charge pump topology for a gate drive high-side power supply," *IEEE Trans. Power Electron.*, vol. 20, no. 2, pp. 300–307, Mar. 2005.
- [5] O. S. Senturk, T. Maerki, P. Steimer, and S. McLaughlin, "High voltage cell power supply for modular multilevel converters," in *Proc. IEEE Energy Convers. Congr. Expo.*, 2014, pp. 4416–4420.
- [6] C. Marxgut, J. Biela, J. W. Kolar, R. Steiner, and P. K. Steimer, "DC-DC converter for gate power supplies with an optimal air transformer," in *Proc. 25th Annu. IEEE Appl. Power Electron. Conf. Expo.*, 2010, pp. 1865–1870.

- [7] R. Steiner, P. K. Steimer, F. Krismer, and J. W. Kolar, "Contactless energy transmission for an isolated 100 W gate driver supply of a medium voltage converter," in *Proc. 35th Annu. Conf. IEEE Ind. Electron.*, 2009, pp. 302–307.
- [8] K. Kusaka, K. Orihara, J.-I. Itoh, K. Morita, and K. Hirao, "Isolation system with wireless power transfer for multiple gate driver supplies of a medium voltage inverter," in *Proc. Int. Power Electron. Conf.*, May 2014, pp. 191–198.
- [9] K. Kusaka *et al.*, "Galvanic isolation system for multiple gate drivers with inductive power transfer—Drive of three-phase inverter," in *Proc. IEEE Energy Convers. Congr. Expo.*, Sep. 2015, pp. 4525–4532.
- [10] J. Pan, F. Qi, H. Cai, and L. Xu, "Efficiency and electromagnetic interference analysis of wireless power transfer for high voltage gate driver application," in *Proc. IEEE Energy Convers. Congr. Expo.*, 2016, pp. 1–5.
- [11] C.-J. Lim and S. Park, "Isolated power supply for multiple gate drivers using wireless power transfer system with single-antenna receiver," *J. Power Electron.*, vol. 17, no. 5, pp. 1382–1390, Sep. 2017.
- [12] M. Takasaki, Y. Miura, and T. Ise, "Wireless power transfer system for gate power supplies of modular multilevel converters," in *Proc. IEEE 8th Int. Power Electron. Motion Control Conf.*, Hefei, China, 2016, pp. 3183–3190.
- [13] F. Lu *et al.*, "A high-efficiency and long-distance power relay system with equal power distribution," *IEEE J. Emerg. Sel. Topics Power Electron.*, to be published, doi: 10.1109/JESTPE.2019.2898125.
- [14] C. Cheng *et al.*, "Load-independent wireless power transfer system for multiple loads over a long distance," *IEEE Trans. Power Electron.*, vol. 34, no. 9, pp. 9279–9288, Sep. 2019.
- [15] C. Cheng, Z. Zhou, W. Li, C. Zhu, Z. Deng, and C. C. Mi, "A multi-load wireless power transfer system with series-parallel-series compensation," *IEEE Trans. Power Electron.*, vol. 34, no. 8, pp. 7126–7130, Aug. 2019.
- [16] W. Zhang and C. C. Mi, "Compensation topologies of high-power wireless power transfer systems," *IEEE Trans. Veh. Technol.*, vol. 65, no. 6, pp. 4768–4778, Jun. 2016.



Chenwen Cheng received the B.S. and Ph.D. degrees in electrical engineering from Zhejiang University, Hangzhou, China, in 2012 and 2017, respectively.

He is currently a Postdoctoral Researcher with San Diego State University, San Diego, CA, USA. His research interests include the motor control, renewable power generation, and wireless power transfer technologies.



Zhe Zhou received the B.E. degree in measure and control technology and instrumentations from the Changchun University of Science and Technology, Changchun, China, in 2011, and the M.S. degree in power electronics and power drives from Tianjin University, Tianjin, China, in 2014.

He is currently with the State Key Laboratory of Advanced Power Transmission Technology, Global Energy Interconnection Research Institute, Beijing, China. His research interests include the applications of the wide-gap device and the power electronic transformer.

include the applications of the wide-gap device and the power electronic transformer.



Weiguo Li received the B.S. degree from Northeast Dianli University, Jilin, China, in 1996, the M.S. degree from China Electric Power Research Institute, Beijing, China, in 2006, and the Ph.D. degree from North China Electric Power University, Beijing, in 2013, all in electrical engineering.

He is currently with the State Key Laboratory of Advanced Power Transmission Technology, Global Energy Interconnection Research Institute, Beijing. His research interests include the

flexible ac transmission systems and power systems.



Zhanfeng Deng received the B.S. and M.S. degrees in welding technology and equipment from Jilin Polytechnical University, Changchun, China, in 1996, and the Ph.D. degree in electrical engineering from Tsinghua University, Beijing, China, in 2003.

He is currently with the State Key Laboratory of Advanced Power Transmission Technology, Global Energy Interconnection Research Institute, Beijing. His research interests include the flexible ac transmission systems and power systems.



Chunting Chris Mi (Fellow, IEEE) received the B.S.E.E. and M.S.E.E. degrees from Northwestern Polytechnical University, Xi'an, China, and the Ph.D. degree from the University of Toronto, Toronto, ON, Canada, in 1985, 1988, and 2001, respectively, both in electrical engineering.

He is a Professor and Chair of Electrical and Computer Engineering and the Director of the Department of Energy—funded Graduate Automotive Technology Education Center for Electric Drive Transportation, San Diego State University (SDSU), San Diego, CA, USA. Prior to joining SDSU, he was with the University of Michigan, Dearborn, from 2001 to 2015.